Mechanical Behaviors of Clay and Sand in terms of Active Soil Skeleton Structure

A. Asaoka[1], T. Noda[1], M. Nakano[1]

Summary

The mechanical differences between sand and clay were examined using the Super/subloading Yield Surface Cam-clay model, which can describe the behaviors of the active soil skeleton structure in terms of a decay of structure, loss of overconsolidation and change of anisotropy with ongoing plastic deformation. Clay was simply and clearly distinguished from sand by the difference in the evolution/degradation rates of structure, overconsolidation and anisotropy. Highly structured overconsolidated clay initially becomes normally consolidated while retaining its structure, and then loses its structure very gradually with continuing plastic deformation. In contrast, loose sand loses its structure very rapidly, while retaining its overconsolidated state. Huge amounts of plastic deformation are required to the case of the loss of overconsolidation in sand. These typical behaviors can be adequately described with a single set of respective material parameters which are not altered depending on their densities.

Introduction

Naturally deposited clays/sands are mostly found in structured states and usually at overconsolidated states. In addition, those soils exhibit more or less anisotropy. In the present study, the mechanical differences between those natural soils are examined employing a modified Cam-clay model with a superloading yield surface [1], a subloading yield surface [2] and rotational hardening [3], by introducing the concepts of soil structure, overconsolidation and stress-induced anisotropy [4] respectively. The evolution laws for these systems are then introduced into the constitutive laws for soils; decay/collapse of the soil structure with ongoing plastic deformation for the superloading yield surface, loss of overconsolidation for the subloading yield surface, and evolution of anisotropy with rotational hardening. This model does not treat the movement of soil particle on a microscopic scale, instead considers the soil skeleton of structure, overconsolidation and anisotropy "in action" from a macroscopic point of view.

Super/subloading Yield Surface Cam-clay Model

The basic concepts of the constitutive model are briefly summarized here.

It is commonly recognized that highly structured soils such as naturally deposited clay or loose sand can have void ratios greater than those possible for the fully remolded soils. This means that under the same stress levels, the structured soils can exhibit a higher void ratio than the remolded soils. Based on this fact, a superloading surface [1] is

[1] Nagoya University, Chikusa, Nagoya, 464-8603, JAPAN

naturally assumed to lie above the Roscoe surface, and this configuration is used to describe the mechanical behavior of structured soils. As the modified Cam-clay model can describe the loading behavior of fully remolded and normally consolidated soil without anisotropy, the superloading surface is assumed to be similar in shape to the Cam-clay yield surface with the origin of the q - p' space as the similarity center, where $p' = -\mathrm{tr}\boldsymbol{T}'/3$ is the mean effective stress of the q - p' space $q = \sqrt{3/2}\|\boldsymbol{S}\|$ is the deviator stress, $\boldsymbol{T}'$ is the effective Cauchy stress tensor with positive tensile components, $\boldsymbol{S} = \boldsymbol{T}' + p'\boldsymbol{I}$ for unit tensor $\boldsymbol{I}$, and the $\|\ \|$ in q represents the Euclidian norm. The Cam-Clay surface is also called the normal-yield surface [2]. The similarity ratio of the Cam-clay surface to the superloading surface in terms of stresses, denoted by R^*, lies between zero and one ($0 < R^* \le 1$). When a current stress state is on the superloading surface, the soil is said to be in a normally consolidated state. For describing the plastic response of structured soils, the flow rule is applied to the superloading surface.

Structured soils, initially on the superloading surface, become overconsolidated when unloading occurs. The soils in such an overconsolidated state, upon subsequent reloading, exhibit elasto-plastic behavior. The plastic response is assumed to satisfy the normality rule associated with the subloading surface [2]. Hence, the current stress state of the overconsolidated soil is always on the subloading surface. The subloading surface is again assumed to be geometrically similar to the superloading surface, and again, the similarity ratio of the subloading surface to the superloading surface in terms of stresses, denoted by R, lies between zero and one ($0 < R \le 1$). The reciprocal $1/R$ corresponds to the overconsolidation ratio (OCR).

As even remolded and normally consolidated soils exhibit anisotropy behavior, the stress ratio parameter $\eta = q/p'$ in the modified Cam clay model is replaced with η^* [4] to describe this effect. Reflecting the above considerations, three loading surfaces are shown in Fig. 1 for an axisymmetric stress state.

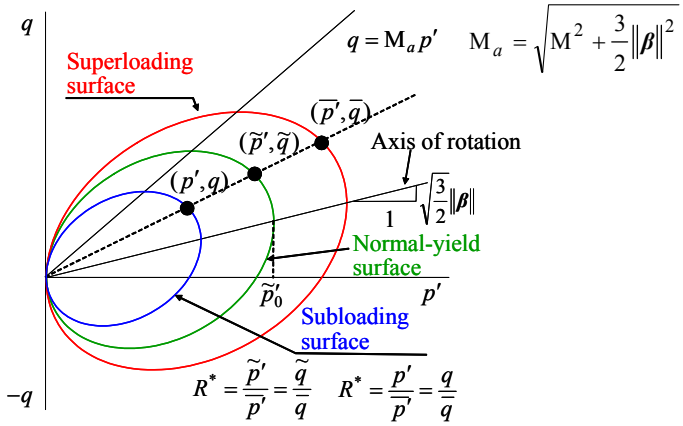

Figure 1: Three loading yield surfaces (after [1])

Since natural soils are generally in a structured overconsolidated state, the current stress state is on the subloading surface as follows.

$$-\int_0^t J\mathrm{tr}\boldsymbol{D}^p d\tau = f(p',\eta^*) + \mathrm{MD}\ln R^* - \mathrm{MD}\ln R$$
$$= \mathrm{MD}\ln\frac{p'}{\tilde{p}'_0} + \mathrm{MD}\ln\frac{\mathrm{M}^2+\eta^{*2}}{\mathrm{M}^2} + \mathrm{MD}\ln R^* - \mathrm{MD}\ln R\,, \tag{1}$$

where $R^* = \tilde{q}/\bar{q} = \tilde{p}'/\bar{p}'$ and $R = q/\bar{q} = p'/\bar{p}'$, and $\bar{q}$, $\bar{p}'$ and $\tilde{q}$, $\tilde{p}'$ are the projected stress parameters on the superloading and normal-yield surfaces, respectively, corresponding to current stress parameters q and p' assuming the similarity center of the three loading surfaces to be the origin of q - p' space. The anisotropy stress ratio parameter is defined by $\eta^* = \sqrt{3/2}\|\hat{\boldsymbol{\eta}}\|$, where $\hat{\boldsymbol{\eta}} = \boldsymbol{\eta} - \boldsymbol{\beta}$, $\boldsymbol{\eta} = \boldsymbol{S}/p'$, and $\boldsymbol{\beta}$ is the rotational hardening tensor [5] representing the rotation of the loading surfaces around the origin of stress space due to induced anisotropy. $\boldsymbol{D}^p$ and $\int_o^t J\mathrm{tr}\boldsymbol{D}^p d\tau$ denote the plastic part of stretching $\boldsymbol{D}$ (with positive tensile components) and the plastic volumetric strain, respectively, and J is the determinant of deformation gradient tensor $\boldsymbol{F}$, expressed as $J = \det\boldsymbol{F} = \mathrm{v}/\mathrm{v}_0$ using the specific volume v(=1+e; e: void ratio) in the current (time t) state and v_0 in the reference (time t = 0) state. The parameter $\tilde{p}'_0$ in Eq.(1) is the mean effective stress on the Cam-clay surface, corresponding to the initial mean effective stress p'_0 in the reference state. M is the critical state constant and D is the dilatancy parameter, related by $\mathrm{D} = (\tilde{\lambda} - \tilde{\kappa})/\mathrm{M}/\mathrm{v}_0$ with the compression index $\tilde{\lambda}$ and the swelling index $\tilde{\kappa}$.

Prager's consistency condition, i.e. taking the time-derivative of Eq. (1), determines the size of the subsequent loading surface and requires the fixing of evolution laws for R, R^* and $\boldsymbol{\beta}$. In the present study, with increasing plastic deformation of the structured overconsolidated soils with induced anisotropy, both R and R^* increase gradually towards one, with $\dot{R}$ and $\dot{R}^*$ positive. Employing the Euclidian norm of plastic stretching $\boldsymbol{D}^p$ and its deviator component $\boldsymbol{D}_s^p$ $(= \boldsymbol{D}^p - 1/3\mathrm{tr}\boldsymbol{D}^p\boldsymbol{I})$ for R, R^* and $\boldsymbol{\beta}$ as the measure of ongoing plastic deformation [1, 2, 3], the evolution laws for sand and clay are given as.

$$\dot{R} = JU\left\|\boldsymbol{D}^p\right\|,\ U = -\frac{m}{\mathrm{D}}\ln R \ \text{(sand and clay)} \tag{2}$$

$$\dot{R}^* = JU^*\sqrt{\frac{2}{3}}\left\|\boldsymbol{D}_s^{\,p}\right\| \ \text{(sand)}, \quad \dot{R}^* = JU^*\left\|\boldsymbol{D}^p\right\| \ \text{(clay)}\,, \quad U^* = \frac{a}{\mathrm{D}}R^{*b}(1-R^*)^c \tag{3}$$

$$\overset{\circ}{\boldsymbol{\beta}} = J\frac{br}{\mathrm{D}}\sqrt{\frac{2}{3}}\left\|\boldsymbol{D}_s^{\,p}\right\|\|\hat{\boldsymbol{\eta}}\|\boldsymbol{\eta}_b\,,\ \boldsymbol{\eta}_b = m_b\frac{\hat{\boldsymbol{\eta}}}{\|\hat{\boldsymbol{\eta}}\|} - \boldsymbol{\beta}\,. \ \text{(sand and clay)} \tag{4}$$

Here, different evolution laws for R^* are used for sand and clay. The degradation parameters m and a, b and c for the overconsolidated state and structured state, respectively, are also different for sand and clay. Here, $\overset{\circ}{\boldsymbol{\beta}}$ is objective rate [5] of $\boldsymbol{\beta}$, m_b is a material constant called the rotational limit surface and br determines the rate of evolution of anisotropy. This law is used for both sand and clay. The differences between

these evolution parameters in Eqs. (2)-(4) describe the difference between the noticeable behaviors of sand and clay as shown below. The details of loading conditions of soils and mechanical features of this model are provided in [1] based on elasto-plastic theory.

The Difference between Clay and Sand

The undrained compression shear behaviors of clay and sand are illustrated in Figs. 2 and 3, as examples of fundamental responses calculated using the constitutive model.

Fig. 1 shows the behaviors of highly structured and heavily and lightly overconsolidated (OC) clay specimens. The material parameters used for simulating clay behavior and the initial conditions for a heavily OC state (i.e., [A] in Fig. 2) are listed in Table 1 and the right side in Fig. 2, respectively. The lightly OC clay was prepared by isotropic consolidation of a clay specimen that had been in a heavily OC state ([A] in Fig. 2) before undrained shearing. The isotropic consolidation was also calculated.

When the lightly OC clay specimen was sheared, softening behavior could be clearly observed accompanying plastic volume compression. In the case of the heavily OC clay specimen, hardening with plastic expansion followed by softening with plastic

Table 1: Material constants for clay

Elasto-plastic parameters		Evolution parameters	
Compression index $\tilde{\lambda}$	0.25	Degradation of structure a (b=c=1)	0.5
Swelling index $\tilde{\kappa}$	0.045	Degradation of overconsolidation m	10.0
Critical state constant M	1.25	Evolution of $\boldsymbol{\beta}$ b_r	0.001
Void ratio at p'=98.1kPa on NCL N	2.73	Limit of rotation m_b	1.0
Poisson's ratio ν	0.3		

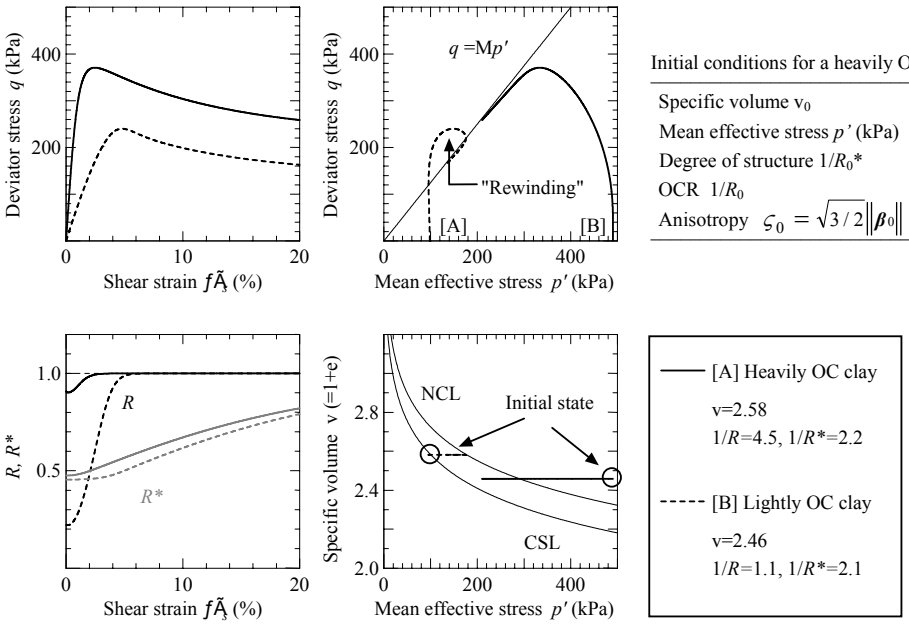

Figure 2: Undrained triaxial compression behaviors of structured and heavily and lightly OC clay specimens

compression, i.e., "rewinding" behavior, was observed, as often seen in natural heavily OC clay [6]. This behavior arises from the fact that the progression of overconsolidation loss proceeds more rapidly than the decay of structure in clay.

Fig. 3 shows the undrained behaviors of five sand specimens. The sand specimens, initially very loose sand ([0] in Fig. 4) were compacted by repeated application of low-level shear stress under drained conditions to achieve different initial compaction states with different densities. Each specimen was then subjected to triaxial undrained shear. The material parameters and initial conditions for the very loose state ([0] in Fig. 4), are listed in Table 2 and the right side of Fig. 3, respectively. In Fig. 4, the repeated application of low-level shear stress under drained conditions yields a huge amount of volume compression, attributable to the rapid collapse of the initial soil structure and a rapid increase in the overconsolidation ratio. Fig. 4 also demonstrates that a wide variety of sand behavior can be adequately described without altering the material constants corresponding to density. The various types of sand behavior are due to the features of structural decay, which progresses more rapidly than the loss of overconsolidation.

Table 2: Material constants for sand

Elasto-plastic parameters		Evolution parameters	
Compression index $\tilde{\lambda}$	0.05	Degradation of structure a (b=c=1)	2.75
Swelling index $\tilde{\kappa}$	0.012	Degradation of overconsolidation m	0.08
Critical state constant M	1.0	Evolution of $\boldsymbol{\beta}$ b_r	3.5
Void ratio at p'=98.1kPa on NCL N	1.97	Limit of rotation m_b	0.7
Poisson's ratio ν	0.3		

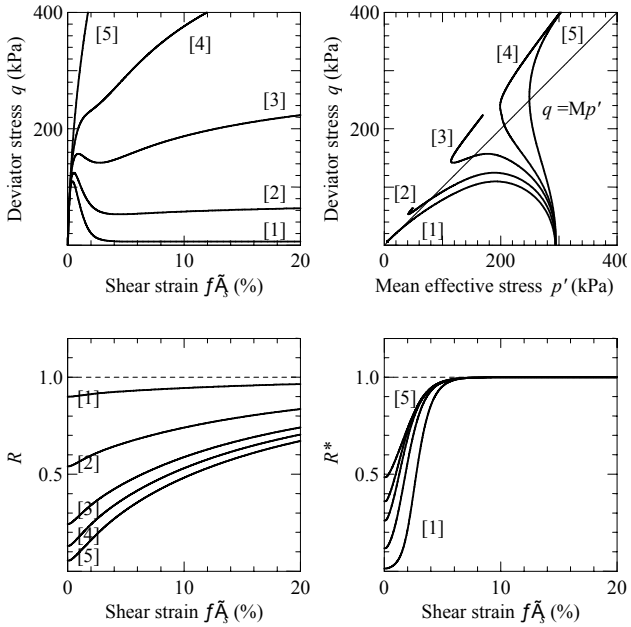

Initial conditions for a very loose state, [0] in Fig. 4.

Specific volume v_0	2.10
Mean effective stress p' (kPa)	294.0
Degree of structure $1/R_0$*	130.0
OCR $1/R_0$	1.0
Anisotropy $\varsigma_0 = \sqrt{3/2}\left\|\boldsymbol{\beta}_0\right\|$	0.0

Figure 3: Undrained triaxial compression behaviors of five sand specimens with different initial densities

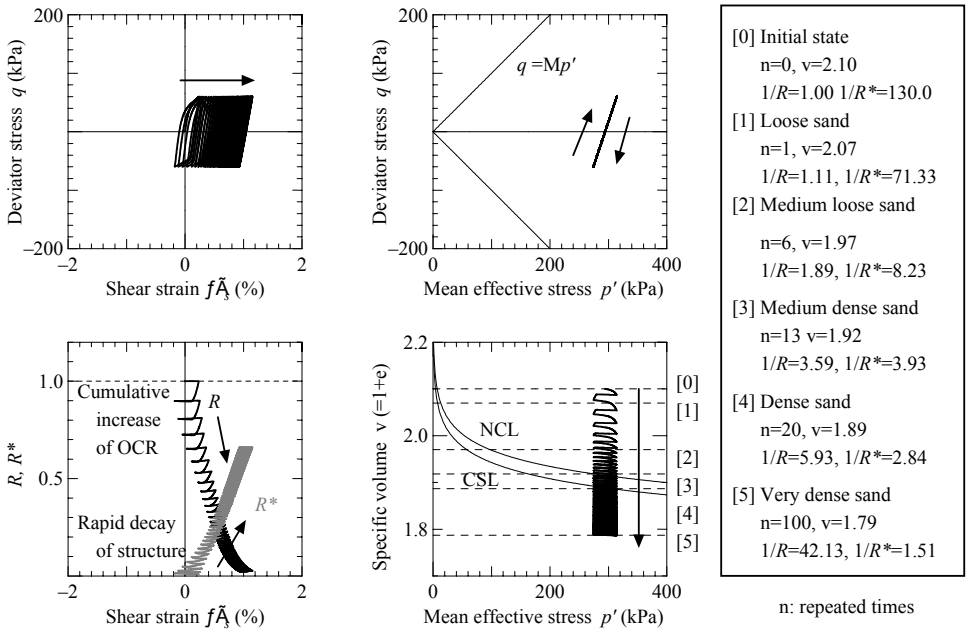

Figure 4: Overall compaction behavior of loose sand under repeated shear stress

Reference

1 Asaoka, A., Noda, T., Yamada, E., Kaneda, K. and Nakano, M. (2002): "An Elasto-plastic Description of Two Distinct Volume Change Mechanisms of Soils", *Soils and Foundations,* Vol.42, No.5, pp. 47-57.

2 Hashiguchi, K. (1978): "Plastic Constitutive Equations of Granular Materials", *Proc. US-Japan Seminar on Continuum Mechanics and Statistical Approaches in the Mechanics of Granular Materials, Sendai*, JSSMFE, pp. 321-329.

3 Hashiguchi, K. and Chen, -Z. P. (1998): "Elasto-plastic Constitutive Equations of Soils with the Subloading Surface and the Rotational Hardening", *Intern. J. Num. Anal. Meth. Geomech.,* Vol. 22, pp. 197-227.

4 Sekiguchi, H. and Ohta H. (1977): "Induced Anisotropy and Time Dependency in Clays", *Constitutive Equations of Soils, Proc. 9th Intern. Conf. Soil Mech. Found. Eng., Spec. Session 9*, *Tokyo*, pp. 229-238.

5 Green, A. E. and Naghdi, P. M. (1965): "A General Theory of an Elastic-plastic Continuum", *Archive for Rational Mechanics and Analysis,* Vol. 18, pp. 251-281.

6 Tatsuoka, F. and Kohata, Y. (1995): "Stiffness of Hard Soils and Soft Rocks in Engineering Applications", *Proc. 1st Intern. Conf. on Pre-failure Deformation Characteristics of Geomaterials*, *Sapporo*, Vol. 2, pp. 947-1063.